This paper was presented in the Space Mechanics Meeting of the AIAA SciTech Forum 2018.

Validated Semi-Analytical Transition Matrices for Linearized Relative Spacecraft Dynamics via Chebyshev Series Approximations

Paulo Ricardo Arantes Gilz*
LAAS-CNRS, Université Paul Sabatier, 31077 Toulouse, France.

Florent Bréhard†
LIP-CNRS, École Normale Supérieure de Lyon, 69364 Lyon, France.
LAAS-CNRS, Université Paul Sabatier, 31077 Toulouse, France.

Clément Gazzino‡
LAAS-CNRS, Université de Toulouse, 31077 Toulouse, France.

During guidance and control procedures of orbiting spacecraft, the respect of positioning and space constraints is decisive for successful missions achievement. The development of algorithms capable of fulfilling these constraints is directly related to how precisely the spacecraft trajectories are known. Since accuracy is essential for these procedures, the prevention and estimation of errors arising from approximations and numerical computations become critical. In this context, we consider solving linear ordinary differential equations via rigorous polynomial approximations in Chebyshev series. These are polynomials together with an error bound accounting for both approximation and rounding errors. Our method allows for the computation of validated approximations of the transition matrices describing the evolution of spacecraft trajectories. The proposed approach is employed in the following applications: first, we consider the linearized impulsive rendezvous framework, demonstrating how to use rigorous polynomials approximations to provide a validated propagation of the relative dynamics between spacecraft; this is then exploited for the hovering phases of the spacecraft rendezvous, where we conceive a validated model predictive control based on semi-definite programs. Finally, we propose a semi-analytical transition matrix for a simplified model of geostationary station keeping, linearizing the spacecraft dynamics which take into account the J2 Earth oblateness effect.

*Ph.D. Graduate, LAAS-CNRS / Université Paul Sabatier, 7 Avenue du Colonel Roche, 31077 Toulouse, France; prarante@laas.fr.
†Ph.D. Graduate, LIP-CNRS / ENS Lyon, 46 Allée d'Italie, 69364 Lyon, France and LAAS-CNRS / Université Paul Sabatier, 7 Avenue du Colonel Roche, 31077 Toulouse, France; florent.brehard@ens-lyon.fr.
‡Ph.D. Graduate, LAAS-CNRS / Université Paul Sabatier, 7 Avenue du Colonel Roche, 31077 Toulouse, France; cgazzino@laas.fr.

It is also available at https://arc.aiaa.org/doi/10.2514/6.2018-1960

I. Introduction

For spacecraft proximity operations (spacecraft rendezvous, station keeping, collision avoidance), the relative dynamics are often linearized for both propagation or control purposes. More specifically, when the magnitude of the relative motion of the spacecraft is small compared to its distance to the Earth, one linearizes the equations of motion, which implies solving simpler linear differential equations. However, no closed form solution is available for these equations in most cases. Exceptionally, for instance, Tschauner-Hempel equations for linearized Keplerian relative motion [1] admit an analytical solution for the transition matrix [2]. For spacecraft station keeping on geostationary Earth orbits (GEO), disturbing effects must be handled. Some models like the CNES Orange model [3] describe the orbital perturbations as the effect of the true geopotential, the lunisolar attraction and the Sun radiation pressure. A transition matrix is not available in this setting, except for the case when considering only the oblateness of the Earth in some cases, for which some analytical methods were developed for the description of the relative motion [4, 5]. However, those methods are not applicable for geostationary spacecraft due to the numerical issues coming from the zero inclination of the reference orbit.

In the general case, the propagation is however performed with numerical iterative schemes (like Euler or Runge-Kutta). The main drawback of this discretization approach is that the number of needed evaluation points can be prohibitive and the discretization error is difficult to estimate precisely. Moreover, for control laws design purposes, analytical solutions are preferable, since various constraints (such as saturation, restricted space regions, etc.) can be satisfied on continuous time domains and not only on discretization grids.

On these lines, an interesting alternative is to obtain polynomial approximations of the solutions because they provide a more compact and accurate approximation and are easier to evaluate and manipulate. Recent works took advantage of such polynomial approximations in the context of model predictive control (MPC) and optimal impulsive constrained control [6, 7]. Their works follow the general framework of semidefinite programming (SDP) based on nonnegative polynomials written as sums of squares (SOS) [8].

The purpose of this article is to present a generic framework and algorithmic tool, which given the linearized equations of relative motion, provides a rigorous semi-analytical transition matrix, expressed as an approximating matrix whose entries are polynomials in Chebyshev basis, and uniform rigorous error bounds for each entry.

From the numerical point of view, spectral methods with Chebyshev expansions used in our work prove to be very efficient and accurate. Other recent works also highlight the advantage of using Chebyshev series expansions in orbital mechanics [9]. They started to successfully replace the classical Taylor series expansions based algebra for intrusive approaches, which has already many applications to astrodynamics and optimal control for proximity operations [10–12].

It is also available at https://arc.aiaa.org/doi/10.2514/6.2018-1960

However, the scope of our work is not limited to numerical efficiency. The contribution of our algorithm is also to provide certified upper bounds for the approximation error (via a Newton-like *a posteriori* validation method), which allows to safely replace the exact solution with polynomials as long as the certified error bound remains smaller than a limit set by the user, depending on the application. This is particularly useful in optimization algorithms for optimal control where a trade-off must be done between low-degree polynomials for efficiency and accurate results.

We employ the proposed algorithm on the study of two heterogeneous examples which allow us to highlight the generality of our approach: one handles the linearized relative motion of a satellite in Keplerian dynamics in low Earth orbit, the other focuses on linearizing relative dynamics in a geostationary orbit. The existing techniques for the computation of the linearized dynamic for the J2 disturbing effect cannot be applied for a GEO spacecraft because the zero inclination of the reference orbit induces numerical issues. Therefore, a state vector composed by the relative orbital elements is used, allowing the propagation of the equation of motion.

Statement of the problem and contributions In the light of the challenges mentioned above, the mathematical problem we want to solve can be stated as follows:

Problem 1 *Consider a d-dimensional order r linear ordinary differential equation (LODE):*

$$X^{(r)}(t) + A_{r-1}(t)X^{(r-1)}(t) + \cdots + A_1(t)X'(t) + A_0(t)X(t) = G(t),$$

over the compact interval $[t_0,t_f]$, of unknown $X : [t_0,t_f] \to \mathbb{R}^d$ and where the $A_i : [t_0,t_f] \to \mathbb{R}^{d\times d}$ and $G : [t_0,t_f] \to \mathbb{R}^d$ are at least Lipschitz-continuous. Call $\Phi(t,t_0)$ the exact mathematical transition matrix.

Provide an approximate transition matrix $\widetilde{\Phi}(t,t_0) \in \mathbb{R}^{rd\times rd}$ and rigorous error bounds $\epsilon_{ij} \geq 0$ $(1 \leq i,j \leq rd)$ satisfying:

$$|\widetilde{\Phi}_{ij}(t,t_0) - \Phi_{ij}(t,t_0)| \leq \varepsilon_{ij}, \qquad 1 \leq i,j \leq d, \quad t \in [t_0,t_f].$$

If the entries of $\widetilde{\Phi}$ are polynomials, we denote each pair $(\widetilde{\Phi}_{ij},\epsilon_{ij})$ as being a Rigorous Polynomial Approximation (RPA) of Φ_{ij} (see [13]).

In Section II, we present the whole method (numerical Chebyshev expansions and *a posteriori* validation) designed to automatically solve Problem 1. This method is fully exposed in [14], and Section II only sketches out the main ingredients in order to give a precise idea of what was implemented, leaving out proofs and technical computations. Section III is devoted to a first application of the method to Tschauner-Hempel equations, which are a rather easy case since dynamics can be decoupled between in-plane and out-of-plane motion and at the end reduced to scalar linear ordinary differential equations. We first show how the method will proceed on this example to output a rigorous

semi-analytical transition matrix; then, we explain how polynomial transition matrices can be employed in the development of a validated MPC for the rendezvous hovering phases. Finally, we perform an *a posteriori* validation to rigorously prove that the final position is reached within accurate precision. Section IV deals with another application: a linearized model for the station keeping of a geostationary satellite, taking into account the J2 perturbation term due to the oblateness of the Earth. In this case, the dynamical system cannot be easily decoupled into scalar differential equations. We will show that our method, generalized to the vectorial case, is able to provide certified and tight error bounds for each component of the motion.

II. Rigorous polynomial approximations of LODE solutions in Chebyshev basis

Since in most cases, exact closed forms solutions of LODE cannot be obtained, a wide variety of numerical algorithms exist for approximating these solutions as accurately as possible. These methods can be divided into two groups:

- *Iterative methods* start at a given initial point with prescribed initial values, and propagate the solution on a time grid using explicit (Euler, explicit Runge-Kutta) or implicit (implicit Runge-Kutta) methods [15].
- On the opposite, *spectral methods* approximate the solution over the global time interval under consideration with a sum of well chosen basis functions, whose coefficients have to be computed [16, 17].

In situations where functions are smooth enough, spectral methods have the advantage over iterative ones of providing a smooth approximation of the solution over the continuous time range, which we can easily derive or integrate for example. For efficiency reasons among others, one often chooses families of polynomials for the basis functions, since addition and multiplication composing them are the basic operations implemented in floating-point units of processors. Besides that, the recent advances in polynomial based optimization methods allowed for very efficient solutions in optimal control problems (see for instance [18, 19] and references therein). In this work, we focus on Chebyshev polynomials, for this family of orthogonal polynomials has very convenient algebraic and approximation properties.

A. Chebyshev approximation theory and numerical solving

1. A short reminder on Chebyshev polynomials and approximation theory

At first glance, working with polynomials in the standard monomial basis and approximating functions with their Taylor development seems to be a convenient choice. In practice, this method goes along with some shortcomings (approximation of non-smooth functions, limited convergence radius due to complex singularities, numerical instability, etc.). For all these reasons, Chebyshev polynomials are preferable in the general case [17].

Here we briefly recall the main properties of Chebyshev polynomials. This family of polynomials is defined by the three-term recurrence $T_{n+2} = 2XT_{n+1} - T_n$ with initial terms $T_0 = 1$ and $T_1 = X$. They satisfy the fundamental trigonometric relation $T_n(\cos\vartheta) = \cos(n\vartheta)$, from which we deduce some of their basic algebraic properties:

$$T_nT_m = \frac{1}{2}(T_{n+m} + T_{|n-m|}), \qquad \left[\frac{T_{n+1}}{2(n+1)} - \frac{T_{n-1}}{2(n-1)}\right]' = T_n \quad (n \geq 2),$$

and that $|T_n(t)| \leq 1$ for $x \in [-1, 1]$.

Endowing the space C^0 of continuous functions over the compact interval $[-1, 1]$ with a Hilbert space structure using the inner product defined by $\langle f, g\rangle = \int_{-1}^{1} f(t)g(t)(1-t^2)^{-1/2}\mathrm{d}t = \int_0^\pi f(\cos\vartheta)g(\cos\vartheta)\mathrm{d}\vartheta$, we see the Chebyshev polynomials as an orthogonal family. To any continuous function f we can associate its Chebyshev coefficients:

$$[f]_0 = \frac{1}{\pi}\int_0^\pi f(\cos\vartheta)\mathrm{d}\vartheta, \qquad [f]_n = \frac{2}{\pi}\int_0^\pi f(\cos\vartheta)\cos(n\vartheta)\mathrm{d}\vartheta \quad (n \geq 1).$$

Hence, the truncated Chebyshev series $f^{[n]} = \sum_{i=0}^{n}[f]_iT_i$ of f is simply the orthogonal projection of f onto the finite-dimensional subspace spanned by $T_0, \ldots, T_n$. Analogously to Fourier series, Chebyshev series have excellent approximation properties [17]. For example, if f is of class C^r over $[-1, 1]$ with $r \geq 1$, then $f^{[n]}$ uniformly converges to f in $O(n^{-r})$. Moreover, at fixed degree n, the n-th truncated Chebyshev series $f^{[n]}$ is a near-best approximation of f among degree n polynomials, with a factor growing relatively slowly, in $O(\log(n))$ [20].

Using these convergence results, one can easily identify a sufficiently smooth function space with the space of corresponding Chebyshev coefficients. Let's call $Ч^1$ the Banach space of continuous functions with absolutely summable Chebyshev series, and define the associated norm $\|f\|_{Ч^1} = \sum_{i\geq 0}|[f]_i|$. We obtain a Banach algebra structure, for we have $\|fg\|_{Ч^1} \leq \|f\|_{Ч^1}\|g\|_{Ч^1}$. Moreover, this norm is a safe overestimation of the supremum norm $\|\cdot\|_\infty$ over $[-1, 1]$:

$$\|f\|_{Ч^1} = \sum_{i\geq 0}|[f]_i| \geq \sup_{-1\leq t\leq 1}\sum_{i\geq 0}|[f]_iT_i(t)| \geq \sup_{-1\leq t\leq 1}|f(t)| = \|f\|_\infty.$$

2. Integral transform, almost-banded structure and efficient numerical solving algorithm

For the sake of clarity, we first focus on the one-dimensional case for Problem 1, that is $d = 1$:

$$x^{(r)}(t) + a_{r-1}(t)x^{(r-1)}(t) + \cdots + a_1(t)x'(t) + a_0(t)x(t) = g(t). \tag{1}$$

over $[t_0, t_f] = [-1, 1]$ (up to a rescaling of the independent variable, if necessary), together with prescribed initial values at -1:

$$x(-1) = v_0, \quad x'(-1) = v_1, \quad \ldots, \quad x^{(r-1)}(-1) = v_{r-1}, \tag{2}$$

where $a_i, g : [-1, -1] \to \mathbb{R}$ are functions in $\mathrm{Ч}^1$ approximated by a truncated Chebyshev series, and $x : [-1, 1] \to \mathbb{R}$ is the unknown function which we want to approximate with a truncated Chebyshev series. For this, a common solution is to rephrase the differential equation (1) into an equivalent integral equation. For instance, as detailed in [14], one considers $\varphi = x^{(r)}$ as the unknown function and expresses lower-order derivatives of x as integrals of φ. This gives:

$$\varphi + \mathbf{K} \cdot \varphi = \psi, \qquad \text{where} \quad \mathbf{K} \cdot \varphi(t) = \int_{-1}^{t} k(t, s)\varphi(s)\mathrm{d}s, \tag{3}$$

with $k(t, s)$ a bivariate polynomial easily computed from the polynomials $a_i(t)$. A symbolic computation shows that for $i \in \mathbb{N}$, $\mathbf{K} \cdot T_i$ is a polynomial with non-zero Chebyshev coefficients between indices 0 and h (initial coefficients) and between $i - d$ and $i + d$ (diagonal coefficients), where the bandwidths h and d directly depend on the maximum degree of the a_i. Hence, the operator $\mathbf{K} : \mathrm{Ч}^1 \to \mathrm{Ч}^1$ has a so-called almost-banded structure [14, 21] in the Chebyshev basis, which is depicted on Figure 1.

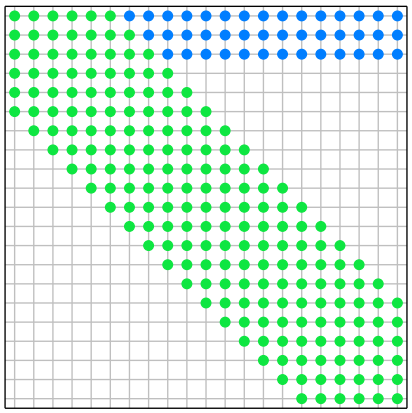

Fig. 1 Matrix representation of $\mathbf{K}$ in Chebyshev basis, truncated at order 20. Almost-banded structure given by initial coefficients (blue) and diagonal ones (green)

Following the general scheme of spectral Galerkin methods [17], we project this problem into finite dimension by taking the truncated operator $\mathbf{K}^{[n]} = \mathrm{п}_n \cdot \mathbf{K} \cdot \mathrm{п}_n$ where $\mathrm{п}_n$ is the orthogonal projection from $\mathrm{Ч}^1$ to the finite-dimensional space spanned by $T_0, \ldots, T_n$. Now, it remains to determine the $n + 1$ first (approximated) Chebyshev coefficients of φ by solving the following finite-dimensional problem:

$$\varphi + \mathbf{K}^{[n]} \cdot \varphi = \psi.$$

Such an almost-banded system is efficiently solved using the algorithm presented in [21]. The mathematical statements and proofs establishing the uniqueness of the solution and the exponential convergence of the numerical truncated solutions to the exact one are to be found in [14].

As a final remark, we note that this method can be extended to the vectorial case, where $X, G : [-1,1] \to \mathbb{R}^d$ and $A_i : [-1,1] \to \mathbb{R}^{d\times d}$. To see this, first notice that the integral transform can be applied as in the scalar case described above. The resulting operator $\mathbf{K} : (\Upsilon^1)^d \to (\Upsilon^1)^d$ is made of $d \times d$ (scalar) integral operators $\mathbf{K}_{ij} : \Upsilon^1 \to \Upsilon^1$ as above (see Figure 2(a)). By rearranging the basis of $(\Upsilon^1)^d$ from $T_0e_1, T_1e_1, T_2e_1, \ldots, T_0e_d, T_1e_d, T_2e_d, \ldots$ to $T_0e_1, \ldots, T_0e_d, T_1e_1, \ldots, T_1e_d, \ldots$, where $(e_1, \ldots, e_d)$ designates the canonical basis of $\mathbb{R}^d$, we end up again with an almost-banded structure depicted in Figure 2(b). Hence, the numerical solving essentially works as in the scalar case.

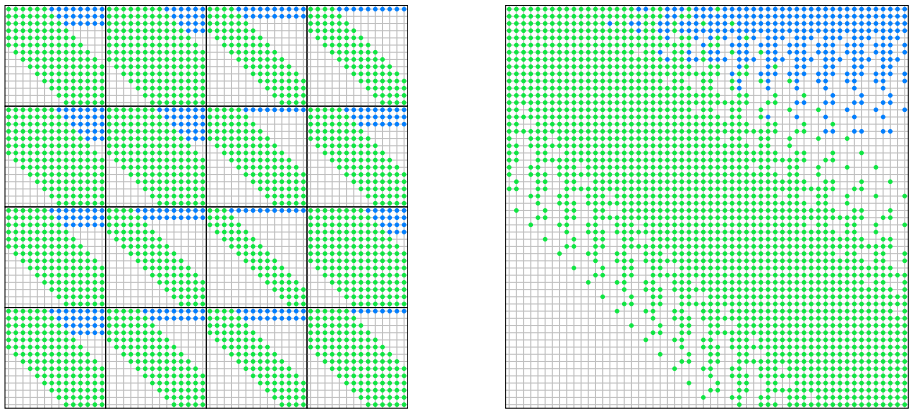

(a) Block matrix representation of vectorial **K**

(b) Almost-banded structure of vectorial **K** in the rearranged basis

Fig. 2 Two representations of vectorial integral operator **K**

B. Validation method

Most of numerical solving methods for differential equations are justified by convergence theorems, estimating how fast the numerical approximations tend to the exact solution when some parameter (number of discretization points, degree of approximating polynomials, etc.) tends to infinity. However, it often appears that these estimates involve non-effective upper bounds (like a bound on the k-th derivative of the solution). Moreover, they do not take into account the inherent rounding errors of floating-point arithmetics. For all these reasons, such convergence results just state that *asymptotically* and for a *sufficiently large* floating-point precision, the solving method is well behaved, but nothing can be said about a particular solution obtained with finite parameters and precision.

The goal of validating techniques is to provide such effective and rigorous error bounds for given approximations. Two main families with different approaches may be distinguished:

- *Self-validating methods* construct an approximation together with a rigorous error bound at one time. A

fundamental example is *interval arithmetics* [22, 23], which consists in replacing real numbers by intervals with floating-point extremities and computing with so-called interval extensions of arithmetic and elementary operations on floating-point numbers. The obtained result is an interval containing the exact mathematical solution. However, in most non-trivial examples, this method fails to produce interesting results (the obtained intervals tend to rapidly become very large). Interval arithmetics is in general a fundamental building block for more elaborate validation methods. For example, in the context of differential equations, combinations of iterative methods and techniques from interval arithmetics give self-validating methods, bounding at each step the error committed at the current discretization point and propagating it for the following ones.

- *A posteriori validation methods* work in two steps. First, the user provides an approximation of the solution, obtained with the procedure of his choice. Then, the validation method computes a rigorous error bound without knowing how this approximation was built.

The paradigm of *a posteriori* validation methods is particularly well suited for spectral methods. Since we explained in the previous section how to compute approximate solutions for LODE (1), we can now suppose that some approximating truncated Chebyshev series is given and focus on the validation method itself.

1. General ideas for designing a posteriori *validation methods*

A wide majority of *a posteriori* validation methods are based on Banach fixed-point theorem and variations around it. Since this article only tackles linear problems, this theorem can be stated in this simplified version:

Theorem 1 *Let $(E, \|\cdot\|_E)$ be a Banach space and $\mathbf{T} : E \to E$ an affine operator whose linear part $\mathcal{D}\mathbf{T}$ is a bounded linear endomorphism. If $\mathbf{T}$ is contracting, that is, if $\|\mathcal{D}\mathbf{T}\|_E = \mu < 1$, then it admits a (necessarily unique) fixed point $x^* \in E$, solution of the equation:*

$$\mathbf{T} \cdot x = x, \tag{4}$$

and for a given $x \in E$, we have the following enclosure for its distance to x^*:

$$\frac{\|x - \mathbf{T} \cdot x\|_E}{1 + \mu} \leq \|x - x^*\|_E \leq \frac{\|x - \mathbf{T} \cdot x\|_E}{1 - \mu}. \tag{5}$$

Hence, designing a fixed-point based validation method for a linear problem of the form $\mathbf{F} \cdot x = y$ essentially boils down to rephrasing it as a fixed-point equation $\mathbf{T} \cdot x = x$ for some contracting affine operator $\mathbf{T}$, which has to be explicitly computable (in order to bound $\|x - \mathbf{T} \cdot x\|_E$) and whose operator norm can be effectively upper-bounded so to obtain a rigorous $\mu < 1$.

A rather generic way to design such a contracting method is to use an adaptation of Newton's method to find zeros of maps [24], which can be used even for non-linear problems. Here we sketch the idea in the linear case. Consider the equation $\mathbf{F} \cdot x = y$, where $\mathbf{F}$ is a linear automorphism. Let $\mathbf{A}$ be an approximation of its inverse $\mathbf{F}^{-1}$. Then the unique solution is also the unique fixed-point of $\mathbf{T}$ defined by:

$$\mathbf{T} \cdot x = x - \mathbf{A} \cdot (\mathbf{F} \cdot x - y), \tag{6}$$

as soon as $\mathbf{A}$ is injective. The underlying idea is that if $\mathbf{A}$ is sufficiently close to the inverse of $\mathbf{F}$, then $\mathbf{T}$ will be contracting.

The remaining work then consists in finding an appropriate $\mathbf{A}$ and bounding the linear part of the resulting $\mathbf{T}$. Such techniques are widely advocated in, for example [24], but quite often, technical tools to design such a Newton operator are treated by hand for precise examples. On the contrary, the method we present below is fully algorithmic over the general case of LODEs and implemented into a C library.

2. Principles of our validation method

Applying variations of Newton's methods to ODEs, even non-linear ones, is not a new idea *per se* (see for examples instructive works [25]). Our method however aims at providing a generic, fully automated and rather efficient algorithm, which could be used as part of a library for rigorous computing as a black box from the point of view of the user.

Considering again the integral reformulation (3) of the problem, we choose a truncation index n and seek an approximate inverse $\mathbf{A}$ of $\mathbf{I}+\mathbf{K}$ as an approximation of the finite-dimensional truncated operator $\mathbf{I}+\mathbf{K}^{[n]}$. Unfortunately, the inverse of this $n+1$ order almost-banded square matrix is dense in general. However, we discuss in [14] the possibility to approximate this inverse with an almost-banded matrix itself.

Having this $\mathbf{A}$ fully determines our Newton-like affine operator $\mathbf{T} : \varphi \mapsto \varphi - \mathbf{A} \cdot (\varphi + \mathbf{K} \cdot \varphi - \psi)$. Its linear part $\mathbf{I} - \mathbf{A} \cdot (\mathbf{I} + \mathbf{K})$ may be bound using the following decomposition of its operator norm:

$$\|\mathbf{I} - \mathbf{A} \cdot (\mathbf{I} + \mathbf{K})\|_{\mathfrak{U}^1} \leq \|\mathbf{I} - \mathbf{A} \cdot (\mathbf{I} + \mathbf{K}^{[n]})\|_{\mathfrak{U}^1} + \|\mathbf{A} \cdot (\mathbf{K} - \mathbf{K}^{[n]})\|_{\mathfrak{U}^1}. \tag{7}$$

- The first term is the approximation error, since $\mathbf{A}$ is only an approximation of $(\mathbf{I} + \mathbf{K}^{[n]})^{-1}$. It boils down to the computation of an $n+1$ order square matrix using multiplications and additions, which is carried out using interval arithmetics to avoid rounding errors.
- The second part is the truncation error, due to the fact that $\mathbf{K}^{[n]}$ is only a finite-dimensional approximation of

K.

The difficulty lies in this second error term, obtained by uniformly bounding $\|\mathbf{A}\cdot(\mathbf{K}-\mathbf{K}^{[n]})\cdot T_i\|_{\mathcal{Y}^1}$ with respect to i. A method for choosing a sufficiently small value of n such that the Newton-like operator $\mathbf{T}$ be contracting, as well as its overall complexity of is given in [14]. While the worst-case bound of n is exponential with respect to the magnitude of the Chebyshev coefficients of a_i, in practice and for a wide range of examples, this method is quite efficient and fully automated.

The sum of these two error terms provides the required Lipschitz constant μ. Next, take φ an approximate truncated Chebyshev series for the exact solution φ^*. Obtaining $\mathbf{T}\cdot\varphi$ and then $\|\varphi-\mathbf{T}\cdot\varphi\|_{\mathcal{Y}^1}$ only requires arithmetic operations for polynomials in Chebyshev basis, plus a multiplication of a vector of coefficients by the matrix $\mathbf{A}$. The computations are rigorously performed using interval arithmetics. Applying Theorem 1, we obtain an upper bound for the approximation error $\varphi-\varphi^*$, for the $\mathcal{Y}^1$-norm, and hence for the uniform norm. Integrating r times φ provides approximations of $x^{*(j)}$ $(0\le j\le r)$, where x^* is the exact solution of (1) with initial conditions (2), together with rigorous error bounds with respect to the uniform norm.

Finally, to solve Problem 1 in the one-dimensional case, the above approximation and validation method is applied r times, for the canonical set of initial conditions. Since the initial conditions appear in the integral equation (3) only in the right-hand side ψ, operators $\mathbf{K}$ and hence $\mathbf{T}$ need to be computed and bounded only once for the r validation processes.

3. Extensions of the method and multidimensional case

In many problems, including the spacecraft dynamics studied in this article, the coefficients and right hand side in LODE (1) are not polynomials but rational functions, special functions, etc. If they belong to $\mathcal{Y}^1$ and are given through truncated Chebyshev series with a certified error bound with respect to the $\mathcal{Y}^1$-norm, then the exact integral operator $\mathbf{K}$ is non-polynomial but well approximated by the polynomial integral operator $\mathbf{K}_P$ obtained by replacing the exact coefficients by their polynomial approximations. An additional term $\|\mathbf{A}\cdot(\mathbf{K}-\mathbf{K}_P)\|_{\mathcal{Y}^1}$ appends to the two others in (7), but the essential ideas of the method remain unchanged.

We also generalized our validation method to the vectorial case ($d>1$ in Problem 1), where the LODE validation tools are easily transposed. An extension of the framework of fixed-point based validation to the vectorial case with individual tight error bounds for each component is currently investigated. A preprint of this work is available here [26].

Another possible improvement concerns generalized boundary values problems (BVP). In the linear case, they can be rigorously solved by computing a basis of certified solutions. However, an *ad-hoc* method for such problems is

preferable, since working with a basis of solutions and recombining them could lead to worse conditioned numerical solutions and overestimated error bounds.

III. Validated linearized impulsive rendezvous and model predictive control

As a first example of application of the method presented in Section II, we consider the impulsive spacecraft rendezvous problem. These missions consist in the execution of a sequence of impulsive maneuvers aiming to bring a follower satellite to the vicinity of a passive target satellite whose trajectory evolves around a central body. The capacity of developing algorithms to address this problem is directly related to how precisely the trajectories developed by each spacecraft involved in the mission are known and, given that precision is a must for these procedures, the prevention and estimation of errors arising from approximations and numerical computations become a critical subject in this context.

Hereafter we describe the mathematical frameworks adopted to model the rendezvous problem. In Fig. 3, the frames used to model the relative motion between the leader S_l and the follower S_f spacecraft are depicted. The Earth-Centered Inertial (ECI) frame is given by $\left\{O, \vec{I}, \vec{J}, \vec{K}\right\}$. The moving Local Vertical / Local Horizontal (LVLH) frame is centered on the leader spacecraft at S_l and given by $\left\{S_l, \vec{x}, \vec{y}, \vec{z}\right\}$ (see [27] for details). Under Keplerian assumptions, the leader orbit is mainly described by its semi-major axis a and its eccentricity $0 < e < 1$. Then, the leader is located on its orbit by the true anomaly ν^*.

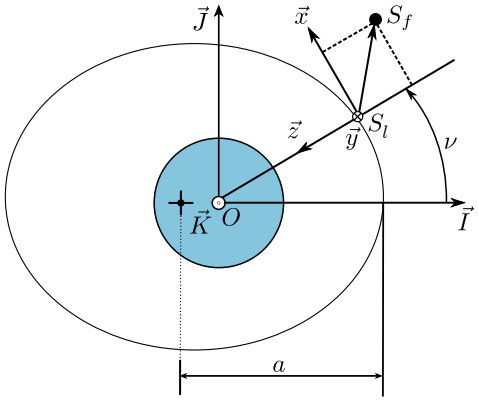

Fig. 3 Inertial and relative frames.

The relative motion is defined as the time history of the relative vector $\overrightarrow{S_l S_f}$. This motion has a state space representation with the following state vector: $X(t) = [x(t),\ y(t),\ z(t),\ \dot{x}(t),\ \dot{y}(t),\ \dot{z}(t)]^T$. Assuming relative navigation hypothesis, $\|\overrightarrow{S_l S_f}\| \ll \|\overrightarrow{OS_l}\|$, a LTV representation for the relative dynamics is obtained: $\dot{X}(t) = A(t)X(t)$

*The true anomaly is in a one-to-one correspondence with time. For the sake of brevity, these variables are interchanged without further remarks in this work.

[28]. By performing the state similar transformation:

$$\bar{X}(\nu) = \mathcal{T}(\nu)X(t), \quad \mathcal{T}(\nu) = \begin{bmatrix} (1+e\cos\nu)\mathbb{I}_3 & \mathbb{O}_3 \\ -e\sin\nu\,\mathbb{I}_3 & \sqrt{\frac{a^3(1-e^2)^3}{\mu(1+e\cos\nu)^2}}\mathbb{I}_3 \end{bmatrix}, \tag{8}$$

where $\bar{X}(\nu) = [\bar{x}(\nu),\, \bar{y}(\nu),\, \bar{z}(\nu),\, \bar{x}'(\nu),\, \bar{y}'(\nu),\, \bar{z}'(\nu)]^T$ and μ is Earth's gravitational constant, the simplified linearized Tschauner-Hempel equations are obtained:

$$\bar{x}''(\nu) = 2\bar{z}'(\nu), \quad \bar{y}''(\nu) = -\bar{y}'(\nu), \quad \bar{z}''(\nu) = \frac{3}{1+e\cos(\nu)}\bar{z}(\nu) - 2\bar{x}'(\nu), \tag{9}$$

where $(\cdot)' = \frac{d(\cdot)}{d\nu}$ and $(\cdot)'' = \frac{d^2(\cdot)}{d\nu^2}$. We observe that the in-plane motion ($\bar{x}$ and $\bar{z}$) is decoupled from the out-of-plane motion ($\bar{y}$). The latter involves only one coordinate and is a simple harmonic oscillator. The former involves two coordinates, but $\bar{x}'$ can be easily eliminated from the equation of $\bar{z}$, which becomes:

$$\bar{z}''(\nu) + \left(4 - \frac{3}{1+e\cos\nu}\right)\bar{z}(\nu) = c, \tag{10}$$

where the constant c is defined from the initial conditions:

$$c = 4\bar{z}(\nu_0) - 2\bar{x}'(\nu_0). \tag{11}$$

First, we analyze precisely in Section A how the method will work on this example in order to produce an approximating Chebyshev expansion of the trajectory and a rigorous error bound. This is done for pedagogical reasons, but in practice the approximation and validation algorithms run as a black box from the point of view of the user. Then, in Section B, we develop a model predictive control algorithm for spacecraft rendezvous hovering phases [7]. The underlying polynomial optimization problem justifies the need for low-degree but still accurate polynomial approximations of the transition matrix. Finally, we use the power of the validation method to perform an *a posteriori* verification of an instance of rendezvous by providing a rigorous enclosure of the chaser's final position. This is particularly important for safety critical missions.

A. Rigorous semi-analytical transition matrix for Tschauner-Hempel equations

Before running the method on LODE (10), we first rescale the interval $[\nu_0, \nu_f]$ to $[-1, 1]$ by introducing the independent variable $\tau \in [-1, 1]$ and letting $\nu(\tau) = \nu_0(1-\tau)/2 + \nu_f(1+\tau)/2 = \omega\tau + \theta$ with $\omega = (\nu_f - \nu_0)/2$,

$\theta = (\nu_0 + \nu_f)/2$, and $Z(\tau) = z(\nu(\tau))$. We obtain:

$$Z''(\tau) + \omega^2 \left(4 - \frac{3}{1 + e\cos\nu(\tau)}\right) Z(\tau) = \omega^2 c, \tag{12}$$

together with rescaled initial conditions:

$$Z(-1) = z(\nu_0), \qquad Z'(-1) = \omega z'(\nu_0).$$

In particular, we observe that the magnitude of the coefficients in Equation (12) grows quadratically with the length of the interval $[\nu_0, \nu_f]$ over which we want to approximate the trajectory.

1. Rigorous approximation of the coefficient

Since the coefficient of Equation (12) is not polynomial, the first step is to provide a rigorous polynomial approximation for it. The cosine function $\tau \mapsto \cos\nu(\tau)$ is approximated by applying our validation method to the harmonic oscillator differential equation:

$$y''(\tau) + \omega^2 y(\tau) = 0, \qquad y(-1) = \cos\nu_0, \quad y'(-1) = -\omega\sin\nu_0. \tag{13}$$

From this, we deduce a rigorous approximation of $\tau \mapsto 1 + e\cos\nu(\tau)$.

Finally, it must be composed with the reciprocal function. Numerical approximations can be obtained using interpolation at Chebyshev nodes, which is a very standard and rather efficient method [17]. Validation is performed through another Newton-like fixed-point method as follows. Let f be a function in $\mathcal{H}^1$, non-zero over $[-1, 1]$, to be inverted, and $g = 1/f$ the solution function. We must solve the functional equation $fg - 1 = 0$ of unknown $g \in \mathcal{H}^1$ (the fact that $g = 1/f$ belongs to $\mathcal{H}^1$ comes from Wiener's Tauberian theorem). If g_0 is a polynomial approximation of g satisfying $\|1 - g_0 f\|_{\mathcal{H}^1} = \mu < 1$, then g is the unique fixed-point of the affine operator $\mathbf{T}$ defined by $\mathbf{T}\cdot g = g - g_0(fg - 1)$ and of Lipschitz constant $\mu < 1$. Hence, Theorem 1 applies and provides an error enclosure for any candidate approximation $\tilde{g}$ of g. Figure 4(a) shows the evolution of the minimal degree p needed to approximate the coefficient $\tau \mapsto \omega^2(4 - 3/(1 + e\cos\nu(\tau)))$ within a $\mathcal{H}^1$-error less than 1, in function of the eccentricity e and the total time interval $[\nu_0, \nu_f]$.

2. Integral transform and numerical solving

Following the integral transform technique described above, we let $\varphi(\tau) = Z''(\tau)$, so that $Z(\tau)$ now becomes:

$$Z(\tau) = Z(-1) + (\tau + 1)Z'(-1) + \int_{-1}^{\tau}\int_{-1}^{s} \varphi(u)\mathrm{d}u = Z(-1) + (\tau + 1)Z'(-1) + \int_{-1}^{\tau}(\tau - s)\varphi(s)\mathrm{d}s.$$

We thus obtain the integral equation:

$$\varphi(\tau) + \int_{-1}^{\tau} \alpha(\tau)(\tau - s)\varphi(s)\mathrm{d}s = \omega^2 c - \alpha(\tau)(Z(-1) + (\tau + 1)Z'(-1)),$$

where $\alpha(\tau) = 4 - 3/(1 + e\cos\nu(\tau))$. For the numerical solving, replace $\alpha(\tau)$ by a polynomial approximation $a(\tau)$ and proceed as in Section B.2: truncate resulting infinite-dimensional equations at a chosen index n and solve the resulting almost-banded system using the algorithm presented in [21] to obtain a degree n polynomial approximation $\tilde{\varphi}$ of the solution.

3. Validation

The validation method we presented in Section B is fully automated. Hence, in this practical example, it suffices to provide to the implemented procedure the differential equation (12) where $\alpha(\tau)$ is given as a polynomial approximation $a(\tau)$ together with the error bound ε, and the candidate polynomial approximate solution $\tilde{\varphi}$ obtained above. The procedure will return a rigorous upper bound of the approximation error, with respect to the Ψ^1-norm.

However, the timings strongly depend on the minimal value for the truncation index that the method finds and which ensures that the obtained operator is contracting. Figure 4(b) gives these values in function of the time interval $\nu_f - \nu_0$ and the eccentricity e of the target reference orbit. We stress out the fact that these values only depend on the equation (that is, ν_0, ν_f and e) and not on the degree of the candidate approximate solution $\tilde{\varphi}$, since the contracting operator $\mathbf{T}$ is completely independent of this approximation.

The results exposed in Figure 4(b) show that a straightforward application of the validation method tends to rapidly become time-consuming after about 10 periods. In next section, we explain how to exploit the periodicity of the equation to validate a freely propagated trajectory over a large number of periods.

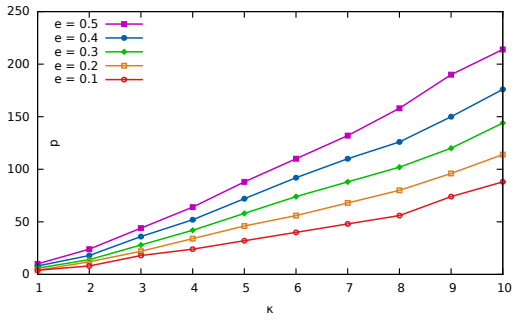

(a) Approximation degree p needed to approximate coefficient $\tau \mapsto \omega^2(4-3/(1+e\cos\nu(\tau)))$ with a $\mathcal{C}^1$-error less than 1

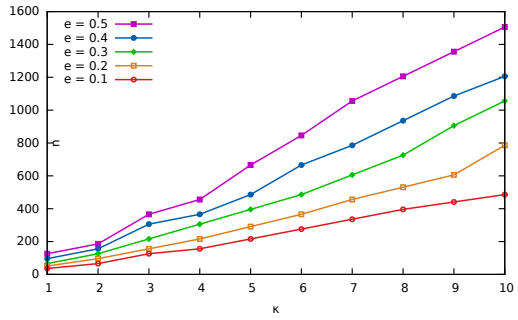

(b) Truncation order n needed to obtain a contracting Newton-like operator for LODE (12)

Fig. 4 Parameters evolution during validation of LODE (12) in function of eccentricity e and total time $[\nu_0, \nu_f] = [0, 2\kappa\pi]$

4. Long-term validated integration techniques

Since Equation (10) is 2π-periodic, validating a transition matrix over $[\nu_0, \nu_0 + 2\pi]$ is a good starting point for most applications. Let

$$\widetilde{\Phi}(\nu,\nu_0) = \left(\begin{array}{c|c|c|c} \tilde{x}_{(i)}(\nu) & \tilde{x}_{(ii)}(\nu) & \tilde{x}_{(iii)}(\nu) & \tilde{x}_{(iv)}(\nu) \\ \tilde{z}_{(i)}(\nu) & \tilde{z}_{(ii)}(\nu) & \tilde{z}_{(iii)}(\nu) & \tilde{z}_{(iv)}(\nu) \\ \tilde{x}'_{(i)}(\nu) & \tilde{x}'_{(ii)}(\nu) & \tilde{x}'_{(iii)}(\nu) & \tilde{x}'_{(iv)}(\nu) \\ \tilde{z}'_{(i)}(\nu) & \tilde{z}'_{(ii)}(\nu) & \tilde{z}'_{(iii)}(\nu) & \tilde{z}'_{(iv)}(\nu) \end{array}\right),$$

where the column of index (i), (resp. (ii), (iii) and (iv)) is a certified approximation of the in-plane trajectory corresponding to the initial conditions $\bar{x}(\nu_0) = 1$ (resp. $\bar{z}(\nu_0) = 1$, $\bar{x}'(\nu_0) = 1$ and $\bar{z}'(\nu_0) = 1$), all the other initial values being set to 0.

To ensure a validated propagation over several periods, the trajectory can be approximated by rigorous piecewise polynomial approximations over each period $[\nu_0 + 2k\pi, \nu_0 + 2(k+1)\pi]$:

$$\begin{pmatrix} \tilde{x}(\nu) \\ \tilde{z}(\nu) \\ \tilde{x}'(\nu) \\ \tilde{z}'(\nu) \end{pmatrix} \in \widetilde{\Phi}(\nu - 2k\pi, \nu_0) J^k \begin{pmatrix} \bar{x}(\nu_0) \\ \bar{z}(\nu_0) \\ \bar{x}'(\nu_0) \\ \bar{z}'(\nu_0) \end{pmatrix}, \tag{14}$$

where $J = \widetilde{\Phi}(\nu_0 + 2\pi, \nu_0)$ is the matrix of rigorous enclosures of the final states after one period. Let us remark that this method does not provide a uniform rigorous polynomial approximation over the whole time interval under

consideration. Moreover, if the entries of J are rather loose intervals, which occurs when $\widetilde{\Phi}(\cdot, \nu_0)$ is made of low-degree polynomial approximations, then the intervals in J^k will rapidly become very large and all precision is lost after a certain number of periods.

In a second step, one can obtain a certified uniform polynomial approximation over the whole time interval if the entries of J^k are sufficiently tight over the required k periods. For that, one uses the numerical polynomial approximation for the trajectory $\bar{X}_{xz}(\nu) = (\bar{x}(\nu), \bar{z}(\nu), \bar{x}'(\nu), \bar{z}'(\nu))$, over $[\nu_0, \nu_f]$, where $\nu_f = \nu_0 + 2\kappa\pi$, obtained in Section A.2. This is validated *a posteriori* by bounding the difference between (14) and the candidate approximation $\bar{X}_{xz}(\nu)$, both considered over each period $[\nu_0 + 2k\pi, \nu_0 + 2(k+1)\pi]$ $(0 \leq k < \kappa)$. To restrict $\bar{X}_{xz}(\nu)$ to a period $[\nu_0 + 2k\pi, \nu_0 + 2(k+1)\pi]$ $(0 \leq k < \kappa)$, note that initially, our method provides a truncated Chebyshev series which is rescaled such that its definition interval is $[-1, 1]$. Hence, for each period, $\bar{X}_{xz}$ must be composed on the right by an affine time rescaling as to extract the desired time subinterval and compare the resulting Chebyshev truncated series with the corresponding precise piecewise approximation. Finally, the sum between the bound of this difference in the $\mathrm{Ч}^1$-norm and the rigorous error bound of the precise solution gives a safe overestimation of the uniform error.

B. Model predictive control for the rendezvous hovering phases using RPA-based transition matrices

Hereafter we focus on the study of the hovering phases of the orbital spacecraft rendezvous missions. The hovering phases are the stages at which the follower satellite is required to remain in the interior of a delimited zone of the space respectively to the target spacecraft. The idea is to provide a validated model predictive control (MPC) algorithm to steer the follower satellite in a fuel-optimal way to the hovering region. The MPC uses *a priori* knowledge about the dynamics of the relative motion between spacecraft to iteratively compute the control corrections that fulfill fuel-optimality and constraints [7, 29].

1. Validated relative dynamics

We consider the previously described states $X(t)$, $\bar{X}(\nu)$ and the relative dynamics given by the simplified linearized Tschauner-Hempel equations in (9). For a given time t (conversely, a true anomaly value ν), the state right after an impulsive velocity correction $\Delta V = [\Delta V_x, \Delta V_y, \Delta V_z]^T \in \mathbb{R}^3$ is defined as $X^+(t)$ and can be computed by:

$$X^+(t) = X(t) + B\,\Delta V(t),\ B = [0_3\ \mathbb{I}_3]^T. \tag{15}$$

Performing the variable changes $X(t) \overset{(8)}{\rightarrow} \bar{X}(\nu)$, the state after the impulse is given by:

$$\bar{X}^+(\nu) = \bar{X}(\nu) + \bar{B}(\nu)\,\Delta V(\nu),\ \bar{B}(\nu) = \mathcal{T}(\nu)\,B. \tag{16}$$

Let be $\bar{\Phi}(\nu_f, \nu_0)$ the real transition matrix of the system of equations (9) from an initial ν_0 to a final ν_f. By considering N impulsive velocities corrections applied at $\nu_1 < \ldots < \nu_N$, the propagation of the state can be formulated as:

$$\bar{X}^+(\nu_N) = \bar{\Phi}(\nu_N, \nu_1)\bar{X}(\nu_1) + \sum_{k=1}^{N} \bar{\Phi}(\nu_N, \nu_k)\bar{B}(\nu_k)\Delta V_k. \tag{17}$$

By applying the Chebyshev series approximation method previously presented, one can obtain rigorous polynomial approximations $\widetilde{\Phi}(\nu, \nu_0)$ on an interval $[\nu_0, \nu_f]$ respecting:

$$|\widetilde{\Phi}_{ij}(\nu_0, \nu) - \bar{\Phi}_{ij}(\nu_0, \nu)| \leq \varepsilon_{ij}(\nu_0, \nu_f), \quad \forall \nu \in [\nu_0, \nu_f]. \tag{18}$$

Then, the propagation of the relative dynamics for $\nu \in [\nu_N, +\infty]$ can be represented by the state $\widetilde{X}(\nu)$, which provides a rigorous approximation of $\bar{X}(\nu)$:

$$\widetilde{X}(\nu) = \widetilde{\Phi}(\nu, \nu_1)\bar{X}(\nu_1) + \sum_{k=1}^{N} \widetilde{\Phi}(\nu_N, \nu_k)\bar{B}(\nu_k)\Delta V_k. \tag{19}$$

2. Propellers, fuel-consumption and saturation

We consider that the follower spacecraft has six identical propellers, one pair symmetrically and oppositely disposed by axis. The fuel consumption is then modeled by sum of the absolute value of the thrusts applied in each direction:

$$\mathcal{J}(\Delta V) = \sum_{i=1}^{N} \|\Delta V(\nu_i)\|_1 = \sum_{i=1}^{N} |\Delta V_x(\nu_i)| + |\Delta V_y(\nu_i)| + |\Delta V_z(\nu_i)|. \tag{20}$$

and assuming that the saturation threshold for each propeller is $\overline{\Delta V} > 0$, this constraint is written as:

$$|\Delta V_x(\nu_i)| \leq \overline{\Delta V}, \qquad |\Delta V_y(\nu_i)| \leq \overline{\Delta V}, \qquad |\Delta V_z(\nu_i)| \leq \overline{\Delta V} \ . \tag{21}$$

3. Space constraints on relative trajectories

During the rendezvous hovering phases, the follower spacecraft is required to steer and remain in the interior of a certain limited region of the space. The idea is to compute a sequence of N velocity corrections generating a relative trajectory that remains inside the hovering region during the interval $[t_N,\ t_{N+1}]$.

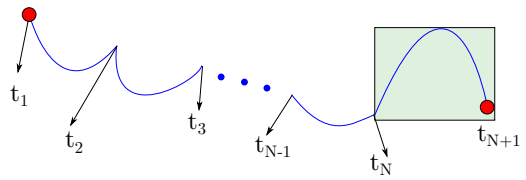

Fig. 5 Steering into the hovering region within N velocity corrections

We assume in the sequel that this hovering range constraint is a rectangular cuboid:

$$x_{\min} \leq x(t) \leq x_{\max} \quad y_{\min} \leq y(t) \leq y_{\max} \quad z_{\min} \leq z(t) \leq z_{\max}, \ \forall t \in [t_N, t_{N+1}]. \tag{22}$$

From (8), we have that:

$$\left[x(t), \quad y(t), \quad z(t)\right] = \underbrace{\frac{1}{1 + e\cos\nu}}_{P(\nu)} \left[\bar{x}(\nu), \quad \bar{y}(\nu), \quad \bar{z}(\nu)\right]. \tag{23}$$

Let us define $\widetilde{P}(\nu) > 0$ a positive RPA of $P(\nu)$ on the interval $[\nu_N, \nu_{N+1}]$ such that $|\widetilde{P}(\nu) - P(\nu)| < \varepsilon_P$, $\forall \nu \in [\nu_N, \nu_{N+1}]$ and the polynomials $\widetilde{P}_x(\nu)$, $\widetilde{P}_y(\nu)$, $\widetilde{P}_z(\nu)$ defined as:

$$\left[\widetilde{P}_x(\nu) \quad \widetilde{P}_y(\nu) \quad \widetilde{P}_z(\nu)\right]^T = \left[\mathbb{I}_3 \quad \mathbb{O}_3\right] \widetilde{X}(\nu). \tag{24}$$

Then, a certified rational polynomial approximation for the LVLH relative positions is given by:

$$\widetilde{x}(t) = \widetilde{P}_x(\nu)/\widetilde{P}(\nu), \quad \widetilde{y}(t) = \widetilde{P}_y(\nu)/\widetilde{P}(\nu), \quad \widetilde{z}(t) = \widetilde{P}_x(\nu)/\widetilde{P}(\nu).$$

The inequalities in (22) can be approximated by:

$$\begin{aligned}
&\widetilde{P}_x(\nu) - \widetilde{P}(\nu)x_{\min} \geq 0, \qquad \widetilde{P}(\nu)x_{\max} - \widetilde{P}_x(\nu) \geq 0, \\
&\widetilde{P}_y(\nu) - \widetilde{P}(\nu)y_{\min} \geq 0, \qquad \widetilde{P}(\nu)y_{\max} - \widetilde{P}_y(\nu) \geq 0, \quad \forall \nu \in [\nu_N, \nu_{N+1}]. \\
&\widetilde{P}_z(\nu) - \widetilde{P}(\nu)z_{\min} \geq 0, \qquad \widetilde{P}(\nu)z_{\max} - \widetilde{P}_z(\nu) \geq 0,
\end{aligned} \tag{25}$$

4. Fuel-optimal impulsive control problem and MPC strategy

Using the mathematical models adopted for the constraints presented in the previous subsections, the fuel-optimal impulsive control problem that is iteratively solved in the model predictive control strategy is formulated as follows:

Problem 2 *Given* $X(\nu_1) \in \mathbb{R}^6$, *N true anomaly firing instants* $\nu_1 < \ldots < \nu_N \in \mathbb{R}^+$, *a true anomaly interval*

$[\nu_N, \nu_{N+1}]$ *find* $\Delta V^* \in [-\overline{\Delta V}, \overline{\Delta V}]^{3N}$ *solution of:*

$$\begin{aligned} &\underset{\Delta V}{\operatorname{argmin}} \quad \mathcal{J}(\Delta V) \\ &s.t. \quad \begin{cases} \widetilde{P}_x(\nu) - \widetilde{P}(\nu) x_{\min} \geq 0, & \widetilde{P}(\nu) x_{\max} - \widetilde{P}_x(\nu) \geq 0, \\ \widetilde{P}_y(\nu) - \widetilde{P}(\nu) y_{\min} \geq 0, & \widetilde{P}(\nu) y_{\max} - \widetilde{P}_y(\nu) \geq 0, \quad \forall \nu \in [\nu_N, \nu_{N+1}]. \\ \widetilde{P}_z(\nu) - \widetilde{P}(\nu) z_{\min} \geq 0, & \widetilde{P}(\nu) z_{\max} - \widetilde{P}_z(\nu) \geq 0, \end{cases} \end{aligned} \tag{$\mathcal{P}.\mathcal{SIP}$}$$

This problem is a semi-infinite program (SIP), since the space constraints must be satisfied for infinitely many values of ν. However, the polynomial inequalities in ($\mathcal{P}.\mathcal{SIP}$) can be converted into so-called linear matrix inequalities (LMIs) using the results on the parametrization of non-negative polynomials on the cone of semi-definite positive matrices presented by Nesterov [8, Theorems 9 and 10], resulting in the semi-definite program (SDP) described in ($\mathcal{P}.\mathcal{SDP}$).

Problem 3 *Given* $X(\nu_1) \in \mathbb{R}^6$*, N true anomaly firing instants* $\nu_1 < \ldots < \nu_N \in \mathbb{R}^+$*, a true anomaly interval* $[\nu_N, \nu_{N+1}]$ *find* $\Delta V^* \in [-\overline{\Delta V}, \overline{\Delta V}]^{3N}$*,* Y_{1w}*,* $Y_{2w} \geq 0$ *solution of:*

$$\begin{aligned} &\underset{\Delta V}{\operatorname{argmin}} \quad \mathcal{J}(\Delta V) \\ &s.t. \quad \begin{cases} \widetilde{p}_{x_{\min}} = \Lambda^*(Y_{1x_{\min}}, Y_{2x_{\min}}), & \widetilde{p}_{x_{\max}} = \Lambda^*(Y_{1x_{\max}}, Y_{2x_{\max}}), \\ \widetilde{p}_{y_{\min}} = \Lambda^*(Y_{1y_{\min}}, Y_{2y_{\min}}), & \widetilde{p}_{y_{\max}} = \Lambda^*(Y_{1y_{\max}}, Y_{2y_{\max}}), \\ \widetilde{p}_{z_{\min}} = \Lambda^*(Y_{1z_{\min}}, Y_{2z_{\min}}), & \widetilde{p}_{z_{\max}} = \Lambda^*(Y_{1z_{\max}}, Y_{2z_{\max}}), \end{cases} \end{aligned} \tag{$\mathcal{P}.\mathcal{SDP}$}$$

where $\widetilde{p}_w$ *is the vector containing the coefficients of the respective non-negative polynomials in the SIP formulation and* Λ^* *is a bilinear operator (see more details in [6, 30]).*

The advantages of reformulating ($\mathcal{P}.\mathcal{SIP}$) are twofold:

- In the SIP formulation, the space constraints are described by infinitely many constraints on the true anomaly, requiring discretization techniques to efficiently compute a “solution". This solution, however, will systematically violate the constraints of the original problem. On the other hand, the SDP formulation provides a finite and exact description of the constraints;
- In previous works [6, 7], SDP solvers were employed in the conception of control strategies for the spacecraft rendezvous problems, showing good performances even in environments with limited computational resources, such as devices dedicated to space applications.

The MPC strategy consists in iteratively solving and updating the inputs of ($\mathcal{P}.\mathcal{SDP}$) in a receding horizon manner. A sequence of N impulsive velocity corrections is computed each time the controller is called, but only the first impulse is applied. Then, the trajectory evolves freely until the next call of the controller (see Fig. 6).

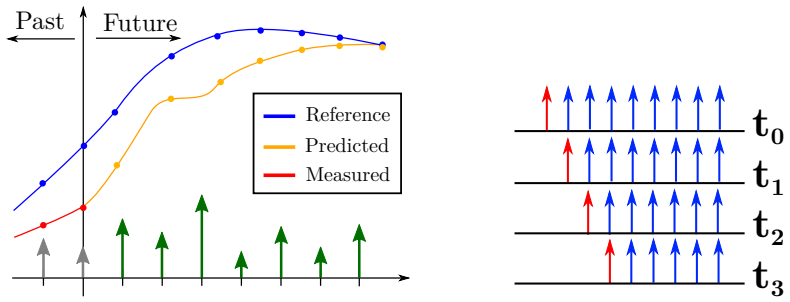

(a) Trajectory evolution and control actions (b) Receding horizon

Fig. 6 Illustration of model predictive control strategy and receding horizon.

5. Simulations and Results

Hereafter we present the results obtained by solving one iteration of the MPC algorithm for the scenario described by the parameters given in Table 1.

Table 1 Scenario parameters

Semi-major axis:	$a = 7011$ km	Eccentricity:	$e = 0.4$
Initial true anomaly:	$\nu_1 = 0$ rad	Number of velocity corrections:	$N = 3$
Interval between impulses:	$\Delta\nu = \pi/4$ rad	Saturation threshold:	$\overline{\Delta V} = 1$ m/s
Initial relative state [m, m/s]:	$[200, 150, 100, 0, 0, 0]$	Degree of RPAs:	5, 7
$[x_{\min}, x_{\max}, y_{\min}, y_{\max}, z_{\min}, z_{\max}]$ [m]:	$[50, 150, -25, 25, -25, 25]$		

The RPAs are computed by a C implementation of the Chebyshev approximation method previously presented. The respective SDP problem is formulated on Matlab via Yalmip [31] (`https://yalmip.github.io/`) and solved using the SDPT3 solver [32] (`http://www.math.nus.edu.sg/~mattohkc/sdpt3.html`). The certificate enclosures are evaluated by treating the bounds of the RPAs via arithmetic interval with the help of the b4m interval arithmetic toolbox library [33] (`http://www.ti3.tu-harburg.de/zemke/b4m/`).

In Fig. 7 the nominal relative trajectory obtained by simply propagating the initial state under the effect of the control actions is presented. Fig. 8, 9 and 10 show the evolution of the x, z and y coordinates of the relative trajectory and their respective certificates.

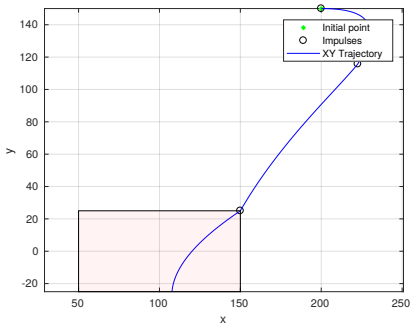

(a) XY-trajectory.

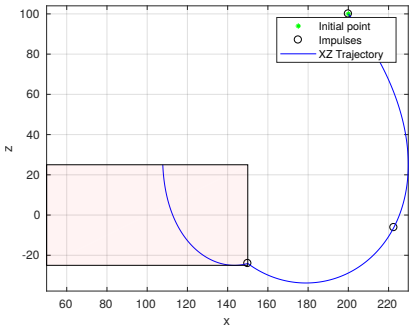

(b) XZ-trajectory.

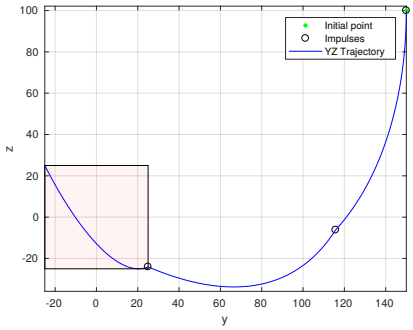

(c) YZ-trajectory.

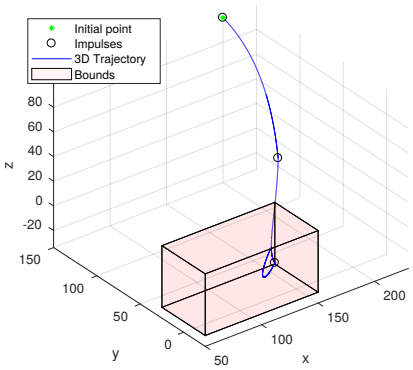

(d) 3D-trajectory.

Fig. 7 Obtained relative trajectory without certification.

The figures from 7(a) to 7(d) demonstrate that the computed impulses produce a relative trajectory that enters the hovering region and remains therein for the imposed true anomaly interval.

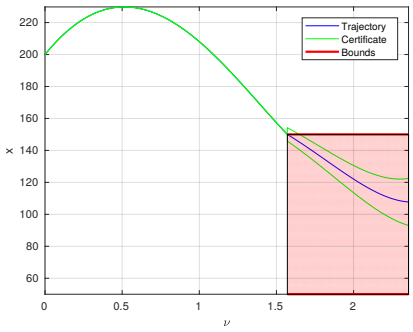

(a) X-trajectory, RPAs of degree 5.

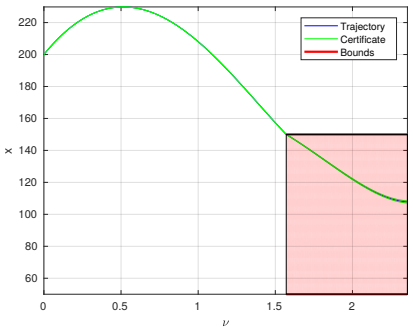

(b) X-trajectory, RPAs of degree 7.

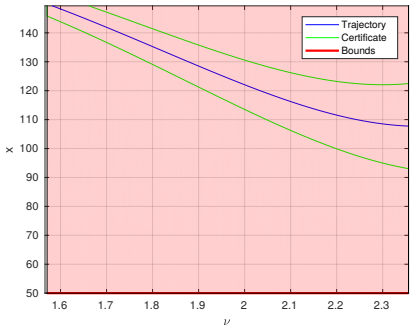

(c) Final uncertainty for x-trajectory, RPAs of degree 5.

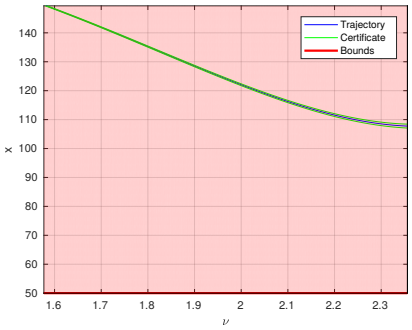

(d) Final uncertainty for x-trajectory, RPAs of degree 7.

Fig. 8 X-coordinate in function of true anomaly for RPAs of degrees 5 and 7.

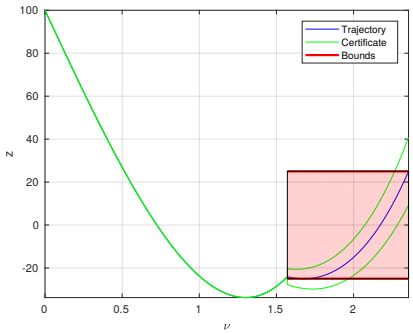

(a) Z-trajectory, RPAs of degree 5.

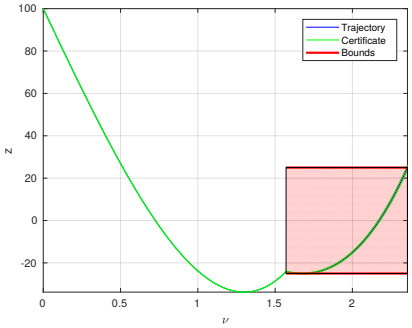

(b) Z-trajectory, RPAs of degree 7.

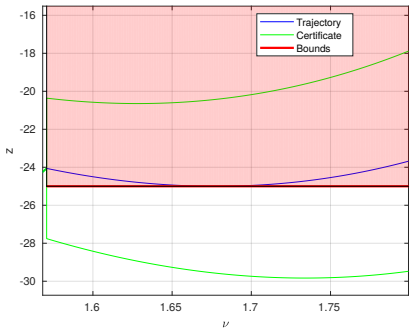

(c) Excursion of z-trajectory, RPAs of degree 5.

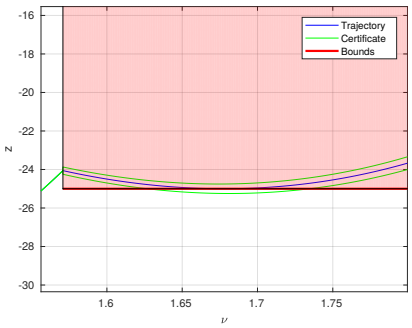

(d) Excursion of z-trajectory, RPAs of degree 7.

Fig. 9 Z-coordinate in function of true anomaly for RPAs of degrees 5 and 7.

We can remark from the figures depicting the evolution of the in-plane x and z coordinates trajectories that the augmentation of the degree of the RPAs produce tighter certificate envelopes (in green) for the errors. This is well illustrated by comparing Fig. 9(c) and 9(d): the RPAs of degree 5 produce a certificate of approximatively 5 m for the excursion of the trajectory, while the RPAs of degree 7 produce a much lower excursion certificate of approximatively

25 cm.

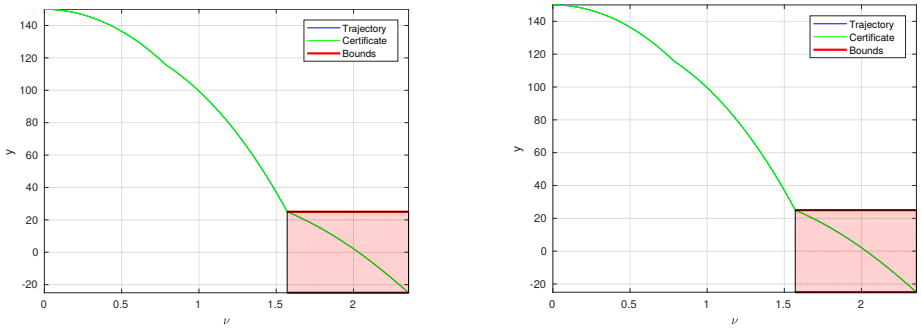

(a) Y-trajectory, RPAs of degree 5.

(b) Y-trajectory, RPAs of degree 7.

Fig. 10 Y-coordinate in function of true anomaly for RPAs of degrees 5 and 7.

From Fig. 10(a) and 10(b) we observe that the certificates for y are tighter than those obtained for the in-plane coordinates x and y (the upper and lower certificates can not even be distinguished without zooming). This is explained by the fact that the out-of-plane dynamics is described by a simpler harmonic oscillator as previously presented in (13), which can be efficiently approximated by low degree polynomials. For instance, the both RPAs produce final certificate enclosure of less than 2 cm for the relative trajectory.

IV. Simple Station keeping of a Geostationary Spacecraft

Telecommunication satellites on a Geostationary Earth Orbit (GEO) have to stay above a fixed point of the Earth, at a position called station keeping position at zero latitude and at a given longitude. However, the geostationary orbit is computed assuming that the Earth produces a central gravitational attraction force. Other forces act on the satellite, such as the real gravitational potential of the Earth, the Sun and the Moon attractions and the Sun radiation pressure. It is therefore mandatory to control the spacecraft trajectory so that it remains in the vicinity of the station keeping point. Among these forces, the so-called J2 disturbing effect of the oblateness of the Earth is the most prominent one for a GEO satellite (see for example [34]) and hence, the study of the integration methods of the equation of the orbital motion perturbed by J2 is of great interest. In this Section, we propose a new integration method for circular and equatorial orbits based on semi-analytical state transition matrix expressed in terms of RPAs (see Section II).

In literature, three categories of integration methods are distinguished cf. [35]. The first category of methods relies on ordinary differential equation models that have to be integrated in order to obtain the spacecraft trajectory. These models consists in finding the relative motion of a spacecraft with respect to a reference point. A big issue in deriving such models is the determination of the angular velocity between the local basis and an inertial one. The references [36] and [37] compute an approximate model by simplifying the expressions of these angular velocities.

The reference [38] simplifies the J2 dynamic equation by averaging the disturbing acceleration over an orbital period. These models are often very complicated and time-varying. The reference [39] uses a coordinate systems based on the gradient of the J2-potential in order to remove the secular drift. Although these dynamics approximations allow for dealing with tractable equations, the state transition matrix remains barely impossible to compute.

The second category of methods aims at computing the perturbed dynamic with differential orbital elements. The references [40] and [4] use a geometric approach to derive the equations for the relative orbital elements. Unfortunately, these results cannot be used because for equatorial orbits, indetermination and numerical problems regarding the inclination of the orbit arise.

The third category of methods deals with the computation of the state transition matrix. The references [5] and [41] compute the state transition matrix for the mean classical orbital elements. Furthermore, the reference [5] derives the successive transformations from the Cartesian position and velocity to the mean orbital elements. As for the second category, the existing methods cannot be used for equatorial orbits because of the numerical problems induced by the zero inclination of the reference orbit.

Our method belongs to the third category and its aim is to compute a state transition matrix with Chebyshev series approximations for a dynamic equation expressed in terms of the relative equinoctial orbital elements. Let us also mention that in this case the linear dynamics system is coupled, which implies that the vectorial case extension of our method is employed.

The J2 perturbation is the C_{20} disturbing term of the decomposition of the Earth gravitational potential Legendre decomposition. This disturbing potential is expressed as:

$$\mathcal{E}_{C20} = \frac{\alpha_{20}}{r^3}\left(\frac{3}{2}\sin^2\varphi - \frac{1}{2}\right), \tag{26}$$

where r is the distance between the center of the Earth and the spacecraft, φ is the geographical latitude and $\alpha_{20} = \dfrac{\mu_\oplus r_\oplus^2 C_{20}}{2}$, $\mu_\oplus$ is the Earth gravitational parameter and $r_\oplus$ the mean Earth radius.

Following the derivation process described in the technical report [42], the disturbing potential is expressed in terms of the Cartesian position in the geocentric inertial reference frame, and then transformed into the equinoctial orbital elements. The differential equation of motion is derived using the Lagrange perturbation theory (see for instance the reference [43]), and then linearized. In Subsection A we give more details on these dynamics for the station keeping of a geostationary satellite with a low-thrust propulsion system, and the linearization we consider. In Section B, we describe a new linearized model for the dynamics expressed with the relative equinoctial orbital elements. Then, in Subsection C, we provide numerical examples for the validated polynomial transition matrices for the linearized dynamics occurring in this perturbed model.

A. Description of the model

The state vector of a satellite orbiting the Earth on a geostationary orbit is described with the equinoctial orbital elements as defined in [43]:

$$x_{eoe} = \begin{bmatrix} a & e_x & e_y & i_x & i_y & \ell_{M\Theta} \end{bmatrix}^T \in \mathbb{R}^6, \tag{27}$$

where a is the semi-major axis, (e_x, e_y) the eccentricity vector components, (i_x, i_y) the inclination vector components, $\ell_{M\Theta} = \omega + \Omega + M - \Theta$ is the mean longitude where Ω is the right ascension of the ascending node, ω is the perigee's argument, M is the mean anomaly and $\Theta(t)$ is the right ascension of the Greenwich meridian.

On top of the Keplerian gravitational attraction produced by the central body supposed to be spherical and homogeneous, spacecraft orbiting the Earth on a GEO orbit undergo orbital disturbing forces. In [44], [45], [46], the potential function of these orbital perturbations is expressed by means of the geographical positions, i.e. radius, latitude and longitude of the spacecraft and the disturbing bodies. As the chosen state vector for the GEO spacecraft is composed of the equinoctial orbital elements, it is mandatory to transform the expression of these potential function in terms of variables of the state vector. In the technical report [42] the geographical position is first transformed in the Cartesian position in the geocentric inertial reference frame referred as the ECI reference frame in [34], and then transformed in the equinoctial orbital elements thanks to conversion formulas derived in the Appendix C of [42].

The disturbing effects described before make the satellite drift away from its nominal position. It is therefore mandatory to equip the satellite with thrusters in order to correct the satellite orbit. These thrusters also create a disturbing acceleration.

With the equinoctial orbital elements as state variables, the dynamic equation to handle the orbital perturbation is given by the Lagrange perturbation technique and the dynamic equation for the effect of the thrusters by the Gauss variation technique (see for instance the references [47] or [48]). By superposition principle, the two effects can be added, leading to the following dynamic equation:

$$\frac{\mathrm{d}x_{eoe}}{\mathrm{d}t} = f_L(x_{eoe}, t) + f_G(x_{eoe}, t)u. \tag{28}$$

where $f_L \in \mathbb{R}^6$ is the Lagrange contribution part of the external forces and $f_G \in \mathbb{R}^{6\times3}$ is the Gauss contribution part. $u = [u_R \; u_T \; u_N]^t \in \mathbb{R}^3$ is the control vector expressed in the local orbital frame.

B. Linearization

For operational purposes, the satellite has to stay on an operating position called station keeping point. As the orbital disturbances induce a drift of the spacecraft position, the thrusters are fired in order to make the spacecraft stay

in the vicinity of its operating position in a so-called station keeping window, whose size is very small with respect to the distance to the Earth. It is therefore possible to linearize the non linear Equation 28 with respect to the orbital elements of the station keeping point:

$$x_{sk} = [a_{sk}\ 0\ 0\ 0\ 0\ \ell_{M\Theta_{sk}}]^t, \tag{29}$$

where a_{sk} is the synchronous semi-major axis and $\ell_{M\Theta_{sk}}$ is the station mean longitude. This station keeping state is a fictitious point evolving on a Keplerian (unperturbed) GEO orbit. It is defined such that the spacecraft mean motion equals the Earth rotation rate. It is then straightforward that:

$$\frac{\mathrm{d}x_{sk}}{\mathrm{d}t} = \begin{bmatrix} 0 & 0 & 0 & 0 & 0 & \sqrt{\dfrac{\mu}{a_{sk}^3}} - \omega_T \end{bmatrix}^T = 0, \tag{30}$$

where ω_T is the Earth rotation rate. Therefore, $a_{sk} = 42164$ km. Moreover, for the simulations, we choose $\ell_{M\Theta_{sk}} = 118°$.

The relative dynamics equations are developed by a new linearization of Equation (28) about the station keeping point (29). Denoting $x = x_{eoe} - x_{sk}$, the relative state model for the SK problem is computed as follows:

$$\frac{\mathrm{d}x}{\mathrm{d}t} = \frac{\mathrm{d}x_{eoe}}{\mathrm{d}t} - \frac{\mathrm{d}x_{sk}}{\mathrm{d}t} = f_L(x_{eoe},t) + f_G(x_{eoe},t)u - 0 \approx f_L(x_{sk},t) + \left.\frac{\partial f_L(x_{eoe},t)}{\partial x_{eoe}}\right|_{x_{eoe}=x_{sk}} x + f_G(x_{sk},t)u. \tag{31}$$

From Equation (31) the dynamical model reads:

$$\frac{\mathrm{d}x}{\mathrm{d}t} = A(t)x + D(t) + B(t)u, \tag{32}$$

where the matrices $A \in \mathbb{R}^{6\times6}$, $B \in \mathbb{R}^{6\times3}$, $C \in \mathbb{R}^{3\times6}$ and $D \in \mathbb{R}^6$ are defined as follows:

$$A(t) = \left.\frac{\partial\left(f_L(x_{eoe}(t),t)\right)}{\partial x_{eoe}}\right|_{x_{eoe}=x_{sk}}, \qquad B(t) = f_G(x_{sk},t), \qquad D(t) = f_L(x_{sk},t). \tag{33}$$

As the the dynamics of the relative equinoctial elements given by the Equation (32) is now linear, the effects of each perturbation can be added together, such that:

$$\begin{aligned} A(t) &= A_{Keplerian}(t) + A_{J2}(t), \\ D(t) &= D_{Keplerian}(t) + D_{J2}(t), \end{aligned} \tag{34}$$

with the exact expression of these matrices available in [42]. From Equations (34) and (32), the (uncontrolled) state transition matrix is computed with our method. In what follows, a numerical integration example is given to show

its effectiveness. Note that this state transition matrix can then be used in the framework of the linear GEO station keeping control problem, which is expressed as an optimal control problem whose objective is to minimize the fuel consumption while ensuring that the relative dynamic is respected and that the spacecraft does not fly out its station keeping window [48], [49] and [50].

C. Numerical example of integration

In this example, the integration has been performed for an initial relative equinoctial orbital elements state:

$$X_0 = \begin{bmatrix} 0 & 10^{-4} & 0 & 10^{-4} & 0 & 0 \end{bmatrix}^T . \tag{35}$$

In Figure 11 the difference between the relative equinoctial elements integrated with the non-linear equation of motion and the linearized equation of motion with the *ode45* function of Matlab is presented on a time interval $[t_0, t_f]$ with $t_0 = 0$ and $t_f = 7$ days. One observes that for the semi-major axis, the two trajectories diverge one from the other up to 0.015 m after seven days. This is due to the fact that the spacecraft moves away from the station keeping point. As for station keeping purposes, a control law will enforce the spacecraft to stay in the vicinity of the station keeping point, the approximation error between the linear and the nonlinear model should remain small. The error between the linear and non linear integration after 7 days is representative of the error that will occur during the station keeping control process because the uncontrolled trajectory flies out the station keeping window after 7 days of free motion.

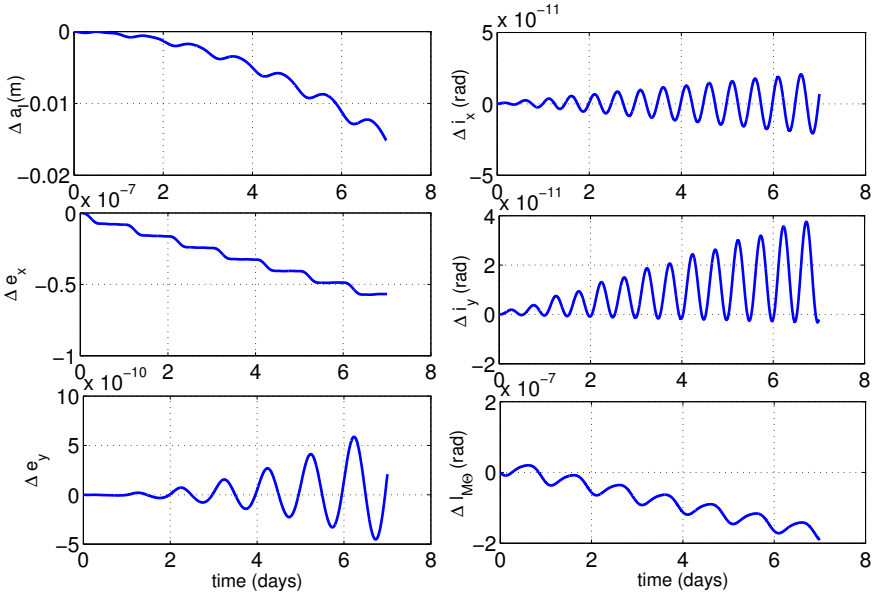

Fig. 11 Error between the integration of the relative equinoctial orbital elements with the non linear and the linearized model.

Based on this, the magnitude of the maximum error obtained between the integrated non-linear equation of motion and the linearized one are heuristically estimated and used as benchmarks in Table 2 in order to compute the minimal

degree of the rigorous polynomial approximations (obtained with our method) which achieve them. Specifically, associated with equation (32), consider the solution $x(t) = \Phi(t,t_0)x_0 + \int_{t_0}^{t} \Phi(t,s)D(s)\mathrm{d}s$, for $t \in [t_0,t_f]$, where $\Phi(t,t_0)$ is the transition matrix and $\int_{t_0}^{t} \Phi(t,s)D(s)\mathrm{d}s$ is a particular solution. The first 6 columns in Table 2 deal with RPAs approximating the transition matrix $\Phi(t,t_0)$. For instance, for the first entry of the transition matrix, a maximum error upper-bound of 10^{-10} requires a degree-26 RPA. Similarly, the last column of Table 2 shows respectively the maximum error upper-bounds and the required degree for RPAs for the particular solution.

i \ j	1	2	3	4	5	6	$\star$
1	10^{-10} : **26**	10^{-7} : **30**	10^{-10} : **37**	10^{-10} : **0**	10^{-10} : **0**	10^{-7} : **0**	10^{-11} : **28**
2	10^{-7} : **33**	10^{-7} : **52**	10^{-7} : **52**	10^{-7} : **0**	10^{-7} : **0**	10^{-7} : **29**	10^{-11} : **51**
3	10^{-10} : **48**	10^{-7} : **52**	10^{-10} : **61**	10^{-10} : **0**	10^{-10} : **0**	10^{-7} : **29**	10^{-11} : **51**
4	10^{-10} : **0**	10^{-7} : **0**	10^{-10} : **0**	10^{-11} : **63**	10^{-11} : **64**	10^{-7} : **0**	10^{-11} : **0**
5	10^{-10} : **0**	10^{-7} : **0**	10^{-10} : **0**	10^{-11} : **64**	10^{-11} : **63**	10^{-7} : **0**	10^{-11} : **0**
6	10^{-10} : **0**	10^{-7} : **0**	10^{-10} : **0**	10^{-11} : **64**	10^{-11} : **63**	10^{-7} : **0**	10^{-11} : **0**

Table 2 Maximum error bounds required for each entry of the transition matrix (columns $j = 1,\ldots,6$) and particular solution (column $j = \star$), and minimal degrees of the rigorous polynomial approximations achieving them, obtained with our method. **Remark:** a null degree indicates a constant entry.

Figure 12 depicts the difference between the relative equinoctial orbital elements computed on one hand by integration of the linearized dynamic given by Equation (32) with the *ode45* function of Matlab and on the other hand by the semi-analytical state transition matrix computed by truncated Chebyshev series as proposed in this paper. The i_y and $\ell_{M\Theta}$ components undergo a secular error whereas the other ones present small periodic errors. Nevertheless, the relative error between these two trajectories is smaller than the error between the linear and the non-linear integration of the trajectory, justifying the use of these state transition matrices as a way to compute the relative trajectory.

V. Conclusion and future developments

An approximation method for obtaining rigorous polynomial approximations of the solutions of LODE via Chebyshev series has been proposed. Extensions for the case in which the coefficients and/or the right hand side of the differential equation are non-polynomial and for the multidimensional case have also been treated. The experimental C source code of the whole method (including the efficient numerical algorithm for Chebyshev expansion of the solution and the automated validation process to certify these approximations) is available here.[†]. Though still being under prototyping, it is totally functional, being used for all the examples illustrating this article.

A validated MPC algorithm for the rendezvous hovering phases has been conceived using the proposed approx-

[†]http://perso.ens-lyon.fr/florent.brehard

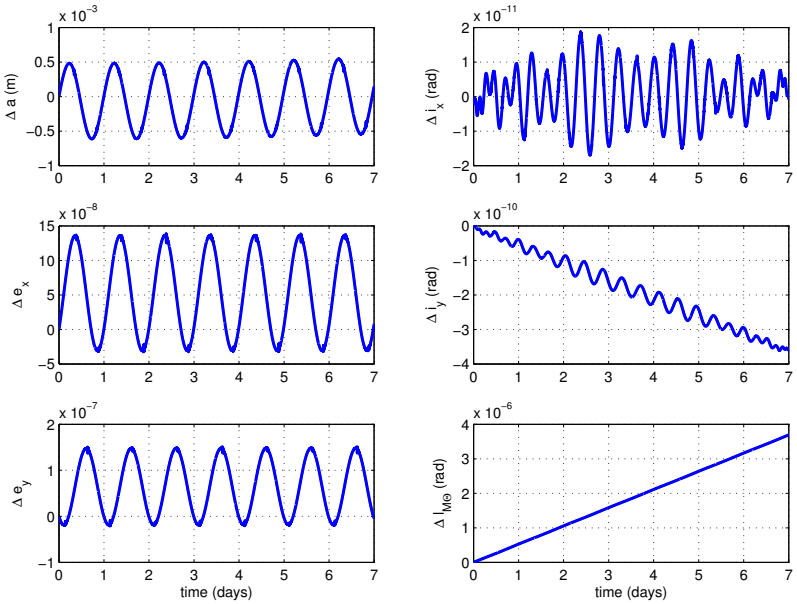

Fig. 12 Error between the integration of the relative equinoctial orbital elements with the *ode45* function of Matlab and the proposed semi-analytical state transition matrix computation method.

imation method. Future experiments would assess the tractability of problem ($\mathcal{P}.\mathcal{SDP}$) on devices dedicated to space applications, focusing on the analysis of the relation between the computational burden and the precision of the polynomial approximations. The study of the performances of problems similar to 4 has already been carried out using an AEROFLEX GAISLER GR-XC6S board containing a synthesized LEON3 microprocessor in [6, 7].

The proposed approximation technique has then been applied on a more complicated case where orbital disturbances arise. Although only the most prominent perturbation has been handled, the proposed state transition matrices computation method could also been applied to other orbital disturbances, as for instance the Sun and Moon gravitation attractions or the Sun radiation pressure. These effects leave room for improvement to our method because it would be necessary to take into account the Sun and Moon positions that are known as tabulated functions. The references [51] or [52] describe how direct collocation methods can be used in order to solve the GEO station keeping optimal control problem. These methods rely on a discretization of the state and control vectors over the time interval $[t_0, t_f]$. The optimal control problem is therefore transformed into a non linear programming problem. The dimension of the unknown vector for the non linear programming problem can be reduced while eliminating the state vector, meaning that the state differential equation of the system must be integrated explicitly. The proposed technique for the computation of the state transition matrix will therefore be used for the integration of the dynamic equation, making the resolution of the GEO station keeping optimal control problem easier.

Another possible extension for this work would be the propagation of uncertain initial conditions via semi-

analytical polynomial transition matrices. When the uncertainties in the initial conditions are not uniformly distributed, we plan consider the generalization to other classes of orthogonal polynomials.

Funding Sources

This work was supported by the FastRelax (ANR-14-CE25-0018-01) project of the French National Agency for Research (ANR), by the French Space Agency (CNES) and Thales Alenia Space.

Acknowledgment

The authors would like to acknowledge Mioara Joldes from LAAS-CNRS and LIP-CNRS for her help as well as her very interesting and useful remarks enhancing the quality and the relevance of this paper.

References

[1] Tschauner, J., and Hempel, P., "Optimale Beschleunigungsprogramme fur das Rendezvous-Manover," *Acta Astronautica*, Vol. 10, No. 5-6, 1964, pp. 296–307.

[2] Yamanaka, K., and Ankersen, F., "New state transition matrix for relative motion on an arbitrary elliptical orbit," *Journal of guidance, control, and dynamics*, Vol. 25, No. 1, 2002, pp. 60–66.

[3] Campan, G., and Brousse, P., "ORANGE: Orbital analytical model for geosynchronous satellite," *Revista Brasileira de Ciencias Mecanicas (ISSN 0100-7386), vol. 16, p. 561-572*, Vol. 16, 1994, pp. 561–572.

[4] Schaub, H., "Relative orbit geometry through classical orbit element differences," *Journal of Guidance, Control, and Dynamics*, Vol. 27, No. 5, 2004, pp. 839–848.

[5] Gim, D.-W., and Alfriend, K. T., "State transition matrix of relative motion for the perturbed noncircular reference orbit," *Journal of Guidance, Control, and Dynamics*, Vol. 26, No. 6, 2003, pp. 956–971.

[6] Deaconu, G., Louembet, C., and Theron, A., "Constrained periodic spacecraft relative motion using non-negative polynomials," *American Control Conference (ACC), 2012*, IEEE, 2012, pp. 6715–6720.

[7] Arantes Gilz, P. R., Joldes, M., Louembet, C., and Camps, F., "Model predictive control for rendezvous hovering phases based on a novel description of constrained trajectories," *IFAC 2017 World Congress, Toulouse, to appear*, 2017. URL `https://hal.laas.fr/hal-01484764`.

[8] Nesterov, Y., "Squared functional systems and optimization problems," *High performance optimization*, Springer, 2000, pp. 405–440.

[9] Riccardi, A., Tardioli, C., and Vasile, M., *An intrusive approach to uncertainty propagation in orbital mechanics based on Tchebycheff polynomial algebra*, Advances in Astrnautical Sciences, AAS/AIAA Astrodynamics Specialist Conference, August 9-13, 2015, Vail, Colorado, U.S.A., American Astronautical Society, 2015, pp. 707–722.

[10] Lizia, P. D., Armellin, R., and Lavagna, M., "Application of high order expansions of two-point boundary value problems to astrodynamics," *Celestial Mechanics and Dynamical Astronomy*, Vol. 102, No. 4, 2008, pp. 355–375.

[11] Lizia, P. D., Armellin, R., Morselli, A., and Bernelli-Zazzera, F., "High order optimal feedback control of space trajectories with bounded control," *Acta Astronautica*, Vol. 94, No. 1, 2014, pp. 383 – 394. doi:http://dx.doi.org/10.1016/j.actaastro.2013.02.011, URL `http://www.sciencedirect.com/science/article/pii/S0094576513000593`.

[12] Di Mauro, G., Schlotterer, M., Theil, S., and Lavagna, M., "Nonlinear control for proximity operations based on differential algebra," *Journal of Guidance, Control, and Dynamics*, Vol. 38, No. 11, 2015, pp. 2173–2187.

[13] Joldeş, M., "Rigorous Polynomial Approximations and Applications," Ph.D. thesis, École normale supérieure de Lyon – Université de Lyon, Lyon, France, 2011. URL `https://tel.archives-ouvertes.fr/tel-00657843`.

[14] Bréhard, F., Brisebarre, N., and Joldes, M., "Validated and numerically efficient Chebyshev spectral methods for linear ordinary differential equations," , May 2017. URL `https://hal.archives-ouvertes.fr/hal-01526272`, preprint.

[15] Iserles, A., *A first course in the numerical analysis of differential equations*, 2nd ed., Cambridge Texts in Applied Mathematics, Cambridge University Press, Cambridge, 2009.

[16] Gottlieb, D., and Orszag, S. A., *Numerical Analysis of Spectral Methods: Theory and Applications*, Vol. 26, Siam, 1977.

[17] Boyd, J. P., *Chebyshev and Fourier spectral methods*, Dover Publications, 2001.

[18] Lasserre, J.-B., *Moments, positive polynomials and their applications*, Vol. 1, World Scientific, 2009.

[19] Claeys, M., Arzelier, D., Henrion, D., and Lasserre, J.-B., "Moment LMI approach to LTV impulsive control," *Decision and Control (CDC), 2013 IEEE 52nd Annual Conference on*, IEEE, 2013, pp. 5810–5815.

[20] Mason, J. C., and Handscomb, D. C., *Chebyshev polynomials*, CRC Press, 2002.

[21] Olver, S., and Townsend, A., "A fast and well-conditioned spectral method," *SIAM Review*, Vol. 55, No. 3, 2013, pp. 462–489.

[22] Moore, R. E., and Bierbaum, F., *Methods and applications of interval analysis*, Vol. 2, SIAM, 1979.

[23] Neumaier, A., *Interval methods for systems of equations*, Cambridge University Press, Cambridge, UK, 1990.

[24] Yamamoto, N., "A numerical verification method for solutions of boundary value problems with local uniqueness by Banach's fixed-point theorem," *SIAM Journal on Numerical Analysis*, Vol. 35, No. 5, 1998, pp. 2004–2013.

[25] Lessard, J.-P., and Reinhardt, C., "Rigorous numerics for nonlinear differential equations using Chebyshev series," *SIAM Journal on Numerical Analysis*, Vol. 52, No. 1, 2014, pp. 1–22.

[26] Bréhard, F., "Fixed-Point Validation with Componentwise Error Enclosures and Application to Coupled Systems of Linear Ordinary Differential Equations," , 2017. URL `https://hal.archives-ouvertes.fr/hal-01654396`, preprint.

[27] Fehse, W., *Automated rendezvous and docking of spacecraft*, Vol. 16, Cambridge university press, 2003.

[28] Tschauner, J., "Elliptic orbit rendezvous," *AIAA Journal*, Vol. 5, No. 6, 1967, pp. 1110–1113.

[29] Arantes Gilz, P. R., and Louembet, C., "Predictive control algorithm for spacecraft rendezvous hovering phases," *Control Conference (ECC), 2015 European*, IEEE, 2015, pp. 2085–2090.

[30] Deaconu, G., "On the trajectory design, guidance and control for spacecraft rendezvous and proximity operations," Ph.D. thesis, Univ. Toulouse 3 - Paul Sabatier, Toulouse, France, Oct. 2013.

[31] Löfberg, J., "YALMIP: A toolbox for modeling and optimization in MATLAB," *Computer Aided Control Systems Design, 2004 IEEE International Symposium on*, IEEE, 2004, pp. 284–289.

[32] Tütüncü, R. H., Toh, K. C., and Todd, M. J., "Solving semidefinite-quadratic-linear programs using SDPT3," *Mathematical programming*, Vol. 95, No. 2, 2003, pp. 189–217.

[33] Zemke, J., "b4m: A free interval arithmetic toolbox for MATLAB," , 1999.

[34] Vallado, D. A., *Fundamentals of astrodynamics and applications*, Space Technology Series, 1997.

[35] Wang, D., Wu, B., and Poh, E. K., "Dynamic Models of Satellite Relative Motion Around an Oblate Earth," *Satellite Formation Flying*, Springer, 2017, pp. 9–41.

[36] Izzo, D., Sabatini, M., and Valente, C., "A new linear model describing formation flying dynamics under J2 effects," *Proceedings of the 17th AIDAA National Congress*, Vol. 1, 2003, pp. 15–19.

[37] Ross, I. M., "Linearized Dynamic Equations for Spacecraft Subject to J˜ 2 Perturbations," *Journal of Guidance Control and Dynamics*, Vol. 26, No. 4, 2003, pp. 657–658.

[38] Schweighart, S. A., and Sedwick, R. J., "High-fidelity linearized J2 model for satellite formation flight," *Journal of Guidance Control and Dynamics*, Vol. 25, No. 6, 2002, pp. 1073–1080.

[39] Morgan, D., Chung, S.-J., Blackmore, L., Acikmese, B., Bayard, D., and Hadaegh, F. Y., "Swarm-keeping strategies for spacecraft under J2 and atmospheric drag perturbations," *Journal of Guidance Control and Dynamics*, Vol. 35, No. 5, 2012, p. 1492.

[40] Schaub, H., and Alfriend, K. T., "J 2 invariant relative orbits for spacecraft formations," *Celestial Mechanics and Dynamical Astronomy*, Vol. 79, No. 2, 2001, pp. 77–95.

[41] Hamel, J.-F., and De Lafontaine, J., "Linearized dynamics of formation flying spacecraft on a J2-perturbed elliptical orbit," *Journal of Guidance Control and Dynamics*, Vol. 30, No. 6, 2007, p. 1649.

[42] Gazzino, C., "Dynamics of a Geostationary Satellite," Tech. rep., LAAS-CNRS, hal-01644934, 2017. URL `https://hal-laas.archives-ouvertes.fr/hal-01644934/document`.

[43] Battin, R. H., *An Introduction to the Mathematics and Methods of Astrodynamics*, Education. AIAA., 1999. doi:10.2514/4.861543.

[44] Shrivastava, S. K., "Orbital Perturbations and Stationkeeping of Communication Satellites," *Journal of Spacecraft*, Vol. 15, No. 2, 1978.

[45] Soop, E. M., *Handbook of Geostationary Orbits*, Kluwer Academic Publishers Group, 1994.

[46] Sidi, M. J., *Spacecraft Dynamics and Control*, Cambridge University Press, 1997.

[47] Zarrouati, O., *Trajectoires spatiales*, cépaduès-e ed., 1987.

[48] Losa, D., "High vs low thrust station keeping maneuver planning for geostationary satellites," Ph.D. thesis, École Nationale des Mines de Paris, 2007.

[49] Gazzino, C., Louembet, C., Arzelier, D., Jozefowiez, N., Losa, D., Pittet, C., and Cerri, L., "Integer Programming for Optimal Control of Geostationary Station Keeping of Low-Thrust Satellites," 2017.

[50] Gazzino, C., Arzelier, D., Cerri, L., Losa, D., Louembet, C., and Pittet, C., "A Minimum-Fuel Fixed-Time Low-Thrust Rendezvous Solved with the Switching Systems Theory," 2017. URL `https://hal.laas.fr/hal-01511019`.

[51] Hull, D. G., "Conversion of optimal control problems into parameter optimization problems," *Journal of Guidance, Control, and Dynamics*, Vol. 20, No. 1, 1997, pp. 57–60.

[52] Betts, J. T., "Survey of numerical methods for trajectory optimization," *Journal of Guidance, Control, and Dynamics*, Vol. 21, No. 2, 1998, pp. 193–207.